Jouini, H.; Mejri, I.; Petitto, C.; Martinez-Ortigosa, J.; Vidal Moya, JA.; Mhamdi, M.; Blasco Lanzuela, T.... (2018). Characterization and NH3-SCR reactivity of Cu-Fe-ZSM-5 catalysts prepared by solid state ion exchange: The metal exchange order effect. Microporous and Mesoporous Materials (Online). 260:217-226. https://doi.org/10.1016/j.micromeso.2017.10.051

Characterization and NH_3-SCR reactivity of Cu-Fe-ZSM5 catalysts prepared by solid state ion exchange: the metal exchange order effect

Houda Jouini[a,*], Imène Mejri [a, b], Carolina Petitto [c], Joaquin Martinez Ortigosa [d], Alejandro Vidal Moya [d], Mourad Mhamdi [a, b], Teresa Blasco [d] and Gérard Delahay [c]

[a]Université de Tunis El Manar, Faculté des Sciences de Tunis, LR08ES01 Laboratoire de Chimie des Matériaux et Catalyse, 2092, Tunis, Tunisie.
[b] Université de Tunis El Manar, Institut supérieur des technologies médicales de Tunis, 1006, Tunis, Tunisie.
[c] Institut Charles Gerhardt Montpellier, UMR 5253, CNRS-UM-ENSCM, Equipe MACS, Ecole Nationale Supérieure de Chimie, 8, rue Ecole Normale, 34296 Montpellier Cedex 5, France.
[d]Instituto de Tecnología Química (UPV-CSIC), Universidad Politécnica de Valencia, Avenida de los Naranjos s/n, 46022 Valencia, Spain.

*Corresponding author. Tel.: +216 99 92 56 55
E-mail address: houda.jouini@fst.utm.tn

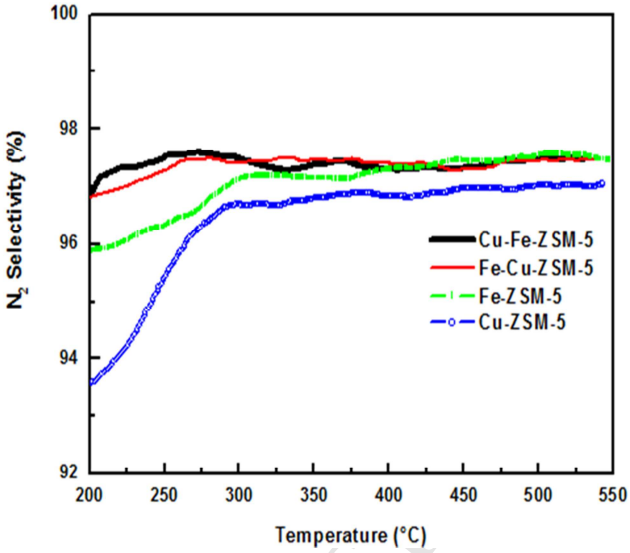

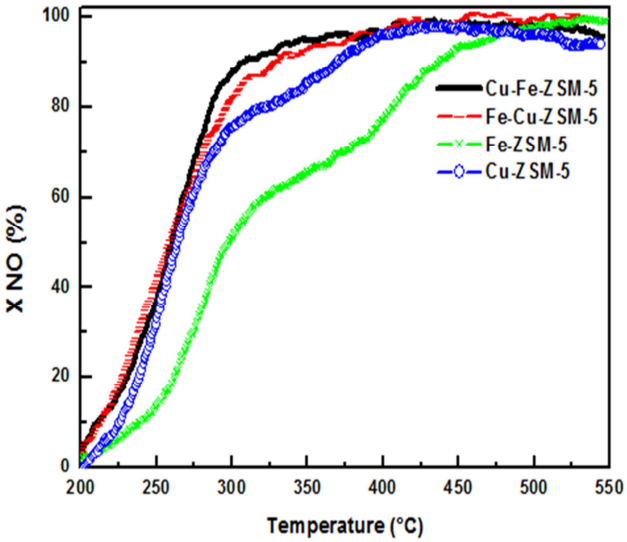

Characterization and NH_3-SCR reactivity of Cu-Fe-ZSM-5 catalysts prepared by solid state ion exchange: the metal exchange order effect

Houda Jouini[a,*], Imène Mejri [a, b], Carolina Petitto [c], Joaquin Martinez Ortigosa [d], AlejandroVidalMoya [d], Mourad Mhamdi [a, b], Teresa Blasco[d] and Gérard Delahay [c]

[a]Université de Tunis El Manar, Faculté des Sciences de Tunis, LR01ES08 Laboratoire de Chimie des Matériaux et Catalyse, 2092, Tunis, Tunisie.
[b]Université de Tunis El Manar, Institut supérieur des technologies médicales de Tunis, 1006, Tunis, Tunisie.
[c]Institut Charles Gerhardt Montpellier, UMR 5253, CNRS-UM-ENSCM, Equipe MACS, Ecole Nationale Supérieure de Chimie, 8, rue Ecole Normale 34296 Montpellier Cedex 5, France.
[d]Instituto de Tecnología Química (UPV-CSIC), Universidad Politècnica de València -Consejo Superior de Investigaciones Científicas, Avda. de los Naranjos s/n, 46022 Valencia, Spain.

*Corresponding author. Tel.: +216 99 92 56 55
e-mail address: houda.jouini@fst.utm.tn

Abstract

The selective catalytic reduction (SCR) of NO with NH_3 in the presence of O_2 and H_2O over a series of Fe and/or Cu-containing ZSM-5 catalysts prepared by solid state ion exchange (SSIE) was investigated. A wide number of experimental techniques (ICP-AES, XRD, HRTEM, ^{27}Al MAS NMR, NH_3-TPD, DRS UV-vis, H_2-TPR and EPR) have been applied to understand the metal exchange order effect on the composition, texture, structure, acidity and speciation of bimetallic materials. DRS UV-vis, H_2-TPR, EPR and HRTEM experiments conducted on Cu-Fe-ZSM-5 and Fe-Cu-ZSM-5 allowed the identification of both isolated and clustered metal species differing in their amount, environment and degree of aggregation leading to a different catalytic behavior of both catalysts.

Keywords: Solid-state ion exchange, Selective catalytic reduction (SCR), NO, ZSM-5.

1. Introduction

Since the beginning of the industrial era, atmospheric pollutants have been continuously rising leading to major threats to environment and human health, and then air pollution control becomes an increasingly important concern worldwide especially in industrialized

countries. The scientific demonstration of the polluting character of different chemical compounds has led to more stringent regulations in order to control their emissions. The contribution of motorized transport in this problem is of paramount interest. The biggest air pollution problems associated with this sector are the emission of unburnt hydrocarbons (HC), carbon monoxide (CO), particulate matter (PM) and nitrogen oxides (NOx) resulting primarily from the spontaneous oxidation of NO. NO_x are highly toxic and harmful gases that contribute to the irritation of the respiratory branches and to the reduction of blood oxygenation power. In the presence of moisture, it turns into nitric acid and participates, under the action of ultraviolet radiation and in combination with VOCs (Volatile Organic Compounds), to the formation of tropospheric ozone. NO_x emissions' control has therefore become one of the greatest challenges for environmental protection, stricter legislations have been enacted and several technologies have been developed and performed to reduce the emissions of NOx including catalytic approaches [1-3]. The selective catalytic reduction (SCR) is considered as one of the most efficient technologies for NO_x removal from stationary sources and vehicles exhaust gas since it operates at lower temperatures than other reduction techniques [4-6]. During the SCR process, NO_x are reduced in the presence of a reducing agent to form innocuous water and nitrogen. Ammonia (urea) is used as a reducing agent mainly for fixed stations (nitric acid plants), however it is also used in catalytic reactors fitted to diesel engines and some vessels because of the high NOx conversions that can be achieved at high space velocity [4]. Mao et al. highlighted the effectiveness of transition metals (Cu^{2+}, Mo^{3+}, Fe^{3+},Cr^{3+}, etc.) exchanged zeolites for NH_3-SCR going far beyond that of commercial vanadia-based catalysts [7], with high activities and nitrogen selectivity on wide temperature ranges and resistance to SO_2 and H_2O at temperature above 450 ºC. Among such a wide family of catalysts Cu-zeolite and Fe-zeolite seem to be particularly interesting for the studied reaction [8]. Delahay et al. have extensively examined both Fe-zeolite and Cu-zeolite

systems [5,9-11]. Zeolites exchanged with iron have been found more active at higher temperatures while those exchanged with copper showed better activity below 300 °C, since above 350 °C, these catalysts are known for NO conversion decline due to the ammonia oxidation phenomenon [12].The identity and nuclearity of Fe and Cu active sites for SCR reaction are still under debate. Chronologically, the first metal-doped zeolite found active in SCR reaction is a zeolite containing copper. Regarding this type of catalyst, it is commonly accepted that the Cu^{2+} ions and copper oxo cations play a crucial role in the NH_3-SCR reaction. Matsumoto et al. studied the NH_3-SCR reaction with a series of ZSM-5 zeolites containing different metal content [13]. They concluded that the main active site is a copper dimer at exchange sites of the catalyst. Kieger et al. also proposed that at temperatures below 300 °C, the active sites in Cu-FAU are formed by neighbouring Cu ions as in the case of $[Cu\text{-}O\text{-}Cu]^{2+}$ dimers. However, above 350 °C all copper ions become active [14]. Among Cu-zeolites, the elaboration of Cu-CHA, has promoted a very intense research activity on the nature of active sites and the reaction mechanisms in the last few years. Now, it is generally assumed that isolated species are also active sites for the NH_3-SCR-NOx reaction [15]. In contrast to Cu-zeolite systems, numerous active sites were nominated for Fe-zeolite system. Several EXAFS studies indicate that the active sites responsible for high SCR activities of Fe-ZSM-5 catalyst are intra zeolite binuclear Fe-oxo [16-18]. Other groups of researchers working on the same catalyst, have proved that active iron sites are: isolated Fe^{2+} and Fe^{3+} ions[19], small Fe_xO_y clusters or oxygen bridged binuclear iron species $[HO–Fe–O–Fe–OH]^{2+}$[20], groups of a wide range of nuclearity and large sets of oxides [21,22]. Alternative suggestions of the active site structure in Fe-ZSM-5 catalyst were also found including Fe_4O_4 groups [23], and oligomeric clusters with low nuclearities containing mononuclear sites [21,24]. However, it was suggested that large oxide particles are fairly inactive [21,25].

At present, most reports are focused on bimetallic exchanged zeolite systems and intensive researches dealt with these promising materials. One of the latest generations of catalysts mentioned for the NH_3-SCR reaction is Fe-Cu-zeolite system. During the last five years, recent studies have revealed that such materials exhibit higher NO conversion activity over a wider temperature range than with individual Fe- and Cu-zeolite catalysts [26-31]. Simultaneous presence of both iron and copper leads to a change of electronic properties, an enhancement of redox ability and a creation of more acid sites than for single metal catalyst.

Herein, we attempt to synthesize a Fe-Cu-catalyst with complementary advantages and synergistic effects of both iron and copper and having the ability to broaden the reaction temperature window. Solid-state ion exchange (SSIE) method has been adopted for catalysts preparation. Our group reported several studies dealing with this technique [32,33], as it shows a relatively simple procedure to obtain a highly exchanged zeolite powder while avoiding the problems of precursors solvation, the influence of the pH and precipitation encountered using wet preparation methods. Furthermore, it is difficult to control the percentage of desired metal-ion exchange in aqueous ion-exchange method. We aimed as well to check the influence of the metal exchange order on the SCR-NO performances and physicochemical properties of a bimetallic ZSM-5 catalyst.

2. Experimental

2.1. Catalysts preparation

Four samples were prepared using commercial zeolite NH_4^+-ZSM-5 (CBV024E, Zeolyst, Si/Al=15) by SSIE method in two steps:

Step 1: 1g of zeolite was finely ground and mixed with the desired amount of anhydrous iron (III) chloride $FeCl_3$ (Sigma- Aldrich, theoretical wt% of Fe =1.5) in an agate

mortar for 5 min under ambient conditions. The resulting mixture was then heated in helium flow (30 cm^3 min^{-1}) for 12h at 290 °C (1 °C min^{-1}).

Step2: the powder obtained from the first step was finely ground and mixed with the desired amount of copper (II) chloride dihydrate $CuCl_2.2H_2O$ (Sigma- Aldrich, theoretical wt% of Cu =1.5) and heated for 12h at 380 °C in helium flow and under the same conditions applied previously. Finally, the catalysts were named as follow: Cu-Fe-ZSM-5 (prepared according to the previous steps), Fe-Cu-ZSM-5 (prepared by the introduction of Cu in step 1 and Fe in step 2), Fe-ZSM-5 (issued from $FeCl_3$ only), and Cu-ZSM-5 (issued from $CuCl_2.2H_2O$ only).

2.2.Activity measurements

The NH_3-SCR of NO catalytic test was performed in temperature programmed surface reaction (TPSR) using a flow reactor operating at atmospheric pressure with a space velocity of 250,000 h^{-1} and a total flow rate of 6 L h^{-1}. 24 mg of each sample (0.025 cm^3) were activated in-situ at 250 °C under oxygen and helium mixture (3.5% H_2O, 8% O_2 and 88.3% He) and then cooled to 50 °C. The samples were tested from 200 °C to 550 °C under the same O_2/He atmosphere and using the following gas composition: 1000 ppm of NO and 1000 ppm of NH_3. The reaction gas mixture is achieved using mass flow meters. The effluent composition was continuously monitored and by sampling on line to a quadruple mass spectrometer (Balzers QMS 200) equipped with Channeltron and Faraday detectors. Catalytic results were expressed as follows:

Conversion of NO: $X_{NO} = \frac{[NO]_0 - [NO]_T}{[NO]_0} \times 100$, where $[NO]_0$ and $[NO]_T$ are the concentrations of NO respectively at the inlet gas reactor and at the temperature T.

2.3.Catalyst characterization

The equipment used for Inductively Coupled Plasma elemental analysis (ICP-AES) was a Varian 715-ES. Before analysis, samples (ca. 20 mg) were dissolved in a HNO_3/HCl/HF solution. The samples crystallinity was checked using a PANanlytical Cubix'Pro diffractometer equipped with an X'Celerator detector and automatic divergence and reception slits using Cu-Kα radiation (0.154056 nm). The equipment is working under a voltage of 45 kV and a current of 40 mA. The diffractograms were recorded in the region of 5-40 ° and were exploited with the software PANalytical X'Pert High ScorePlus. The phase identification was accomplished by comparing the experimental diffractograms with the references of the international database ICDD (The International Centre for Diffraction Data). HRTEM observations were performed using a JEOL-JEM 2100F instrument equipped with an X-MAX microanalysis detector and operating under an accelerating voltage of 200 kV and an energy resolution of 20 eV.^{27}Al MAS NMR spectra were recorded at room temperature on a Bruker WB spectrometer with a frequency of 104.21 MHz and using $Al(NO_3)_3.9H_2O$ as a reference material. The excitation pulse and recycle time were 6 ms and 0.06 s, respectively. An overall 4096 free induction decays were accumulated. The NH_3-TPD experiments were performed on a Micromeritics Autochem 2910 apparatus analyzer equipped with an on-line thermal conductivity detector. The reactor was placed in a programmable oven and the temperature monitoring is set using a thermocouple placed in contact with the material. Each sample (50 mg) is first pretreated for 1h at 500 °C under a flow of 20%O_2/80%N_2 with a heating rate of 10 °C min^{-1} and a flow rate of 30 cm^3 min^{-1}. Solid is then cooled to 100 °C under helium stream and ammonia (5% NH_3/He) is adsorbed at this temperature for 45 minutes to saturation. Purging with helium is carried out at 100 °C during 1h, then the thermal desorption is performed up to 600 °C using a heating rate of 10 °C min^{-1} and a flow rate of 30 cm^3 min^{-1}. UV-Vis DRS measurements were performed on a Perkin Elmer Lambda 45

spectrophotometer equipped with a diffuse reflectance attachment. Spectra were recorded at room temperature in the wavelength range of 200-900 nm using $BaSO_4$ as reference material. H_2-TPR profiles were obtained on an automated Micromeritics Autochem 2920 analyzer. Before H_2-TPR measurements, samples (50 mg) were pretreated in a quartz U-tube reactor under 5%O_2/He flow (30 cm^3 min^{-1}) at 500 °C (10 °C min^{-1}) for 30 mn and then cooled under helium to 40 °C. The samples were then reduced from 40 °C to 800 °C (5 °C min^{-1}) under 5%H_2/Ar atmosphere (30 cm^3 min^{-1}). EPR spectra were recorded at 105 K on a Bruker EMX-12 spectrometer operating in the X band with a frequency and an amplitude modulation of 100 kHz and 1.0 Gauss respectively.

3. Results

3.1.NH_3-SCR catalytic activity

The prepared catalysts were tested in the SCR of NO with ammonia and the collected results were shown in Fig.1.Table 1 summarizes the reaction temperatures of tested catalysts corresponding to 50% (T_{50}) and 100% (T_{100}) of conversion and the operating temperature window (temperature range corresponding to 100% of conversion).

Fig.1. NO conversion over prepared catalysts.

Fig.1 shows the SCR window of Fe-ZSM-5which is limited with approximately 100% of conversion starting from 451°C. This behaviour is characteristic of Fe-zeolite system which demonstrates a maximum activity at high temperatures [20,34], while Cu-ZSM-5 exhibits a good catalytic performance at low temperatures reaching 50% of conversion at 267 °C versus 288 °C for Fe-ZSM-5 catalyst. A slight decline in NO conversion starting from 450 °C was detected which is not related to the deterioration of the catalyst. In fact, this decline is due to the unselective oxidation of ammonia to NO schematized as: $4\ NH_3 + 5\ O_2 \rightarrow 4\ NO + 6\ H_2O$ [35].

Table 1: SCR operating temperatures.

Cu-Fe-ZSM-5 and Fe-Cu-ZSM-5 seem to have the same catalytic profile apart from a slight difference in the catalytic behaviour between Cu-Fe-ZSM-5 and Fe-Cu-ZSM-5 from 280 to 375 °C (the maximum difference is of 5±1 %). Fig. 2b shows that both bimetallic catalysts exhibit the same concentration of N_2O^+ fragment while in the case of Cu-Fe-ZSM-5, the formation of NO_2 is more pronounced. This finding reveals a different catalytic behaviour of these catalysts despite the close conversion values later.

Fig. 2.Evolution of N_2O^+ fragment (m/e=44) (a) and NO_2^+ fragment (m/e=46) (b) intensities over Cu-Fe-ZSM-5 and Fe-Cu-ZSM-5 catalysts.

3.2.ICP-AES chemical analysis results.

The chemical analysis was performed by ICP-AES technique. Obtained results are gathered in Table 2 including Cu and Fe contents and Si/Al molar ratio. The examination of this table shows that Si/Al atomic ratios correspond to the data provided by the zeolite manufacturer (Zeolyst). Iron and copper amounts are slightly higher for Cu-Fe-ZSM-5 (wt%(Fe)= 1.24 and wt% (Cu)=1.48) than for Fe-Cu-ZSM-5 (wt%(Fe)= 1.16 and wt% (Cu)=1.36).Copper contents in all catalysts are very close to the theoretical amount set for the preparation of catalysts (1.5 wt%). This result is expected since the SSIE method is the most convenient to introduce precise amounts of metals. However, iron contents are found to be lower. Metal loss during heat treatment is possibly due to the volatilization of some iron species. Ion exchange degree (ED) was determined using ICP-AES results and the obtained values were presented in Table 2. ED values indicate that bimetallic solids were over exchanged (ED>100 %). This over-stoichiometry is explained by the fact that in MFI-type zeolites, the position of tetrahedrally coordinated Al^{3+} ions are spatially highly separated as reported Kouwenhoven [36].

Table 2: ICP-AES chemical analysis results of as-synthesized materials.

3.3.XRD and HRTEM results

Parent zeolite diffractogram is identical to that illustrated in the "Collection of Simulated XRD Powder Patterns for Zeolites" [37]. All the characteristic peaks corresponding to the parent zeolite have appeared in the XRD diffractograms of prepared samples evidencing the stability of zeolite structure after the SSIE process. The principal diffraction peaks intensities of the parent zeolite decreased with metals addition due to the higher absorption coefficient of copper and iron compounds for the X-ray radiation [38].

Peaks matching with the PDF reference patterns revealed the presence of F_2O_3 (ICDD PDF#33-0664), CuO (ICDD PDF#48-1548) and Fe_2CuO_4 (ICDD PDF#33-0664) phases over Cu-Fe-ZSM-5 and Fe-Cu-ZSM-5 solids although oxide peaks were not detected in the samples diffractograms. This is due to the low amount of metals introduced in the zeolites (around 1wt %) which is in the limit of detection of the XRD equipment, besides the fluorescence of metals (especially iron) which considerably decreases the peaks intensity of the oxide particles. The small size of oxide nanoparticles provides broad XRD peaks, which overlap with those of MFI-type zeolite since it exhibits many peaks over the entire 2θ range.

Fig. 3 shows HRTEM micrographs of studied samples. The distribution of copper and iron species were confirmed by EDX elemental analysis showing that highly dispersed nano-sized metal species (<100 nm) were formed. The size of the particles leads us to speculate that they are on the outer surface of the zeolite [39]. HRTEM image of Fe-ZSM-5 (Fig. 3a) indicates the presence of few iron oxides particles (8-10 nm) while in the case of Cu-ZSM-5 (Fig. 3b), smaller copper oxide particles are present on the surface of the solid with an homogeneous distribution and a size between 3 and 9 nm.

Fig. 3. HRTEM-STEM micrographs of Fe-ZSM-5 (a), Cu-ZSM-5 (b), Cu-Fe-ZSM-5 (c) and Fe-Cu-ZSM-5 (d).

The HRTEM image of Cu-Fe-ZSM-5 (Fig. 3c) shows nanosized copper particles of 9-24 nm with a rather uniform distribution. A limited number of large iron particles (spectrum 9) appear with a size up to 60 nm. In the case of Fe-Cu-ZSM-5 (Fig. 3d), iron particles are present with a smaller size (8-20 nm). They coexist with smaller Fe-Cu nanocomposites (spectra 3 and 4) as confirmed by EDX analysis with an average size of 6 nm. It can be reasonable to conclude that copper addition promotes the aggregation of iron species in Cu-Fe-ZSM-5 while iron reduces the aggregation of copper particles by forming Fe-Cu nanocomposites.

3.4.^{27}Al MAS NMR results

^{27}Al MAS NMR spectroscopy was conducted to investigate the change in aluminium coordination after steam treatment of SSIE. The spectra of NH_4^+-ZSM-5 and prepared solids are presented in Fig.4. All samples exhibit a sharp dominant resonance at around 54 ppm assigned to tetrahedrally coordinated Al in lattice positions (framework Al). The intensity of this peak is reduced after metal loading, probably due to the presence of paramagnetic Fe^{3+} and Cu^{2+} cations [40]. This may also suggest that the loading of Fe and/or Cu distorted the framework Al species coordination environments, making some of them NMR-silent due to their lower symmetry [17]. A small contribution at 0 ppm assigned to Al in octahedral symmetry, indicates the presence of extra-framework aluminium (EFAL) even in the parent zeolite, although its relative contribution is larger on exchanged ZSM-5. The intensity of EFAL peak is higher in the case Cu-Fe-ZSM-5 than in the other samples evidencing that a probable dealumination has occured.

Fig.4. ^{27}Al MAS NMR spectra of NH_4^+-ZSM-5 and issued catalysts.

3.5.NH_3-TPD

It is of interest to examine changes in the surface acidity of the zeolite support due to metal loading since catalyst acidity plays an important role in promoting its catalytic performance [41,42].Temperature programmed desorption of NH_3 (NH_3-TPD) experiments were carried out on the prepared samples to determine the amount and strength of their different acid sites. The desorption temperatures determined from the NH_3-TPD analysis and the corresponding amounts of ammonia consumption are presented in Table 3. TPD profiles of NH_4^+-ZSM-5 and issued solids are shown in Fig.5a. Fig.5b displays peak deconvolution using a Gaussian fit of Cu-Fe-ZSM-5 TPD profile. The pure zeolites profile is similar to that described in the literature for the MFI structure [43,44]. It shows two well resolved desorption peaks located respectively at 217 and 458 °C. The low temperature peak (peak-l) corresponds to the desorption of weakly chemisorbed ammonia on Lewis and/or weak Brönsted acid sites [45], or silanol groups [43]. The high temperature peak (peak-h) is assigned to the desorption of strongly chemisorbed ammonia on strong Brönsted acid sites (Si-OH^+-Al) [44].Loading of Cu and/or Fe appeared to introduce an additional desorption peak located at intermediate temperature (peak-i). Such a peak is attributed to ammonia desorption from medium-strength acid sites. Examination of Table 3 reveals that the strength of this acidity in Cu-Fe-ZSM-5 is slightly higher than that in Fe-Cu-ZSM-5 as indicated by the position of the maximum temperatures at 275 and 269 °C, respectively.

Fig.5. NH_3-TPD profiles of NH_4^+-ZSM-5 and prepared catalysts (a) and deconvolution of Cu-Fe-ZSM-5 TPD profile (b).

Incorporation of Fe and/or Cu into NH_4^+-ZSM-5 decreased its total acidity, evidencing that metal ions consume the acid sites of the parent zeolite. Following the works of Jentys et al.[46], the percentage of loss in strong Brönsted acid sites has been evaluated (Table 3) showing a significant consumption of these sites by the iron species. NH_3 desorption from Cu-ZSM-5 solid between the range 250-300 °C was correlated to NH_3 desorption occurring from

Cu-NH_3 complex [47]. The "h" peak maximum temperature of Cu-ZSM-5, Cu-Fe-ZSM-5 and Fe-Cu-ZSM-5 shifted towards a lower temperature which may be due to a decrease in Brönsted acid sites density whereas that of Fe-ZSM-5 shifted to higher temperature. This is probably related to ammonia adsorption on iron ions, which are able to bind two molecules of NH_3 (Fe binuclear hydroxo species) [34].

Table 3: NH_3-TPD and H_2-TPR results.

3.6.DRS UV-vis spectroscopy

In order to investigate the nature of metallic species in the prepared samples, DRS UV-vis spectroscopy experiments were conducted. The Kubelka-Munk function was calculated from the measured reflectance and the results are shown in Fig.6. However, it was difficult to quantify the obtained metal species as their extinction coefficients is unknown and several peaks overlap. Fe-ZSM-5 spectrum (Fig.6a), reveals the presence of a band around 270 nm arising from isolated mononuclear Fe^{3+} sites in octahedral coordination [48], whereas bands at $300 < \lambda < 400$ nm are assigned to octahedral Fe^{3+} in small oligomeric Fe_xO_y clusters [49].

Diffuse reflectance UV-vis studies on Cu-ZSM-5 have been reported (Fig.6b). Besides the fundamental absorption bands of the zeolite matrix located at 271 and 287 nm [50,51], the band appearing at 331 nm was attributed to Cu(II)-O^- electronic transition species [52]. Unreacted $(CuCl)_n$ clusters is demonstrated by the presence of the absorption edge at about 384 nm [53].The presence of Cu-O-Cu entities were reported only for the over-exchanged Cu-zeolites and not for Cu-ZSM-5 with Cu/Al < 0.5 [54].

Fig. 6. DRS UV-vis spectra of Fe-ZSM-5 (a), Cu-ZSM-5 (b), Cu-Fe-ZSM-5 and Fe-Cu-ZSM-5 (c).

UV-vis spectra of Cu-Fe-ZSM-5 and Fe-Cu-ZSM-5 are shown in Fig.6c. Both Cu-Fe-ZSM-5 and Fe-Cu-ZSM-5 exhibit same UV-vis bands with a slight blue shift for Fe-Cu-ZSM-5 due to the difference in the metallic species environment.

Cu-Fe-ZSM-5 spectrum showed the band of isolated Fe^{3+} in octahedral coordination, at 270 nm, and the same band appeared at 267 nm in the case of Fe-Cu-ZSM-5. Oligonuclear $Fe^{3+}{}_xO_y$ clusters were characterized by bands located in the range of 300-400 nm. The band appearing in Cu-Fe-ZSM-5 spectrum at 327 nm (323 nm for Fe-Cu-ZSM-5) may be ascribed also to Cu^{2+} species.

3.7.H_2-TPR

Presence of transition metal cations introduces redox properties in a catalyst which are considered as critical settings that determine the degree of NO conversion of SCR catalysts [14,55]. The influence of the amount and the nature of metal cations on redox properties of the above catalysts are evaluated by H_2-TPR technique.

With performing a blank run with unexchanged zeolite, no H_2 uptake was detected. TPR profiles of Cu-ZSM-5 and Fe-ZSM-5 are shown in Fig.7. H_2 consumption amounts calculated for both samples are gathered in Table 3.

TPR profile ofCu-ZSM-5 deconvolution (Fig.7b) shows three reduction peaks centered at 371, 478and 620 °C. As demonstrated by Delahay et al. [56], the copper reduction process involves the following steps:

$$CuO + H_2 \rightarrow Cu^0 + H_2O \quad (1)$$

$$Cu^{2+} + 0.5H_2 \rightarrow Cu^+ + H^+ \quad (2)$$

$$Cu^+ + 0.5H_2 \rightarrow Cu^0 + H^+ \quad (3)$$

Reactions (1) and (2) occur at lower temperature than reaction (3). It was also found that bulk CuO exhibits one reduction peak at around 277 °C (550 K) [56], thus, we assigned the two peaks below 500 °C to the reduction of Cu^{2+} into Cu^+ (H_2/Al= 0.51 and 07.4 respectively).

The latter peak is attributed to the reduction of Cu^{+} species located in different positions into Cu^{0} as speculated the H_2/Cu ratio determined from the quantitative study.

Fig. 7. H_2-TPR profiles of Fe-ZSM-5 (a), Cu-ZSM-5 (b), Cu-Fe-ZSM-5 and Fe-Cu-ZSM-5 (c).

According to the literature [57], two main reduction zones can be defined for TPR profile of Fe-ZSM5 in order to differentiate iron oxide aggregates from iron cationic species. The first peak centred at around 300-400 °C is ascribed to the reduction of Fe (III) species in extra framework positions into Fe (II) oxidation state. Peaks above 450 °C correspond to the reduction of Fe(II)O iron oxide species in Fe^{0}. H_2-TPR profile of Fe-ZSM-5 (Fig.7a) can be decomposed in two peaks at 357 and 581 °C using a Gaussian fit analysis. The first peak is attributed to the reduction of Fe^{3+}species located in different positions into Fe^{2+} (H_2/Fe> 0.5). The second peak is attributed to the reduction of iron oxide to metallic iron. It can be concluded that in our case, iron species in single metal catalyst seem to be more easily reducible compared to copper species.

Concerning bimetallic samples, the deconvolution of corresponding spectra was very difficult as some iron and copper species are reduced at close temperatures. Recorded spectra consisted of several overlapped peaks. They were fitted with linear background and Gaussian convolution shapes. Obtained results show that multiple copper and iron species coexist in each sample where the assignment of H_2 consumption peaks was a difficult task and only tentative assignments were done relying on the literature. TPR spectra of Cu-Fe-ZSM-5 and Fe-Cu-ZSM-5 are presented in Fig.7c. With reference to the works of Zhang et al. dealing with Fe-Cu-MFI system [26], peaks at 219 and 228 °C for Cu-Fe-ZSM-5 and Fe-Cu-ZSM-5 respectively were ascribed to the reduction of isolated Cu^{2+} ions. Those at 359 and 367 °C were attributed to the reduction of Fe^{3+} and/or Fe_2O_3 to Fe^{2+}. Peaks above 500 °C are ascribed to the reduction of reduction of Fe^{2+} and/or FeO to Fe^{0}. H_2-TPR results clearly show that

copper species were easily reduced in bimetallic solids. Both Cu and Fe reduction peaks shifted to higher temperatures when inversing the metal exchange order, suggesting that this parameter plays a role in the redox ability of the studied samples.

3.8.EPR results

Since EPR is a powerful technique for analysing the state of iron and copper ions [58], it was conducted to characterize our catalysts. Fig.8 shows their EPR spectra recorded at 105 K while Table 4 gathers the results of the EPR quantitative study.

Fig. 8. EPR spectra of prepared catalysts.

EPR spectrum of Fe-ZSM-5 shows three signals at effective g-values of 2, 4.3 and 6 which are known from earlier studies [19,59]. These signals can be assigned to Fe^{3+} of FeO_x clusters, isolated Fe^{3+} ions in tetrahedral coordination, and in environments with more neighbouring oxygen ions (5 or 6), respectively. In the EPR measurement, the Fe^{2+} species that was bonded to the ZSM-5 framework was not detected because the iron ions observed in various zeolite systems are usually in the high spin $3d^5$ configuration [60]. Cu-ZSM-5 sample exhibit an axial EPR spectrum of isolated Cu^{2+} ions with resolved hyperfine structure (HFS) with $g_{\parallel}$= 2.38 and $g_{|}$= 2.09. Cu-Fe-ZSM-5 and Fe-Cu-ZSM-5 spectra also revealed the two signals of isolated Cu^{2+} and that of isolated Fe^{3+} in tetrahedral coordination at g=4.3. The latter signal is much more intense in the case of Fe-Cu-ZSM-5. The relative concentration of copper, determined from double integration of the EPR signals, is found to be 2 , 1. 2 and 1 for Cu-ZSM-5, Fe-Cu-ZSM-5 and Cu-Fe-ZSM-5 respectively. For these samples, it is difficult to discriminate the Fe^{3+} of FeO_x cluster signal due to the similar region with that of $g_{|}$ of isolated Cu^{2+}. Cu-Fe-ZSM-5 showed an additional signal appearing at g= 9.3 which arise from isolated Fe^{3+} sites in strong rhombic or axial distortion environment [59], while

Cu-Fe-ZSM-5 EPR spectrum reveals the presence of highly coordinated ferric ions at g=5.6 and g=6 [39].

Table 4: EPR quantitative study.

4. Discussion

Solid-state ion exchange (SSIE) typically yields high metal loadings approximating the amounts set theoretically. Furthermore, it is easy to control the metal exchange degree in this preparation method. Solids prepared with SSIE leads to the formation of both atomically dispersed metal ions and oxide nanoparticles [20]. Cu-ZSM-5 catalyst showed higher NO conversion at low-temperature region compared to Fe-ZSM-5. The slight decrease in NO conversion above 450 °C on Cu-ZSM-5 might be explained by the high activity of Cu species for the oxidation of ammonia's undesired reaction. This behaviour is mainly attributed to small CuO particles detected during HRTEM observations. Fe-ZSM-5 catalyst is found more active at high-temperature region confirming the fact that NH_3 adsorption on Fe active sites in such material inhibits its SCR activity at low temperatures leading to lower NO conversion compared to Cu-ZSM-5 system [61]. Bimetallic catalysts exhibit a better low temperature conversion compared to Cu-ZSM- 5. This finding is in accordance with TPR results since it was found that the presence of Cu along with Fe leads to a better reducibility compared to single Cu-ZSM-5 suggesting an interaction between iron and copper species. The presence of such easily reducible copper species is responsible of enhancing low temperature conversions by oxidizing NO to NO_2 and nitrates, known as rate controlling intermediate species of low temperature SCR-NO reaction [27]. TPR also showed that metallic species reduction occurs at lower temperatures in the case of Cu-Fe-ZSM-5 compared to Fe-Cu-ZSM-5. Reduction peaks shift to higher temperatures when inversing the metal exchange order, suggesting that this parameter plays a role in the redox ability of studied samples. The easier is the reduction of

metal species, the higher is its oxidation ability in the SCR-NO reaction. This fact was confirmed by the higher concentration of formed NO_2^+ fragment over Cu-Fe-ZSM-5.

Acidity is one of the important parameters that rule the catalytic performances over zeolite-based catalysts. Results of NH_3-TPD showed that prepared samples exhibit weaker total acidity compared to parent zeolite indicating that catalysts acidity is not very implied in determining their catalytic activities in SCR reaction.

According to ICP-AES elemental analysis, the catalyst Fe-Cu-ZSM-5 showed a slight loss in metal contents (1.36 wt% of Cu and 1.16 wt% of Fe) versus Cu-Fe-ZSM-5 catalyst (1.48 wt% of Cu and 1.24 wt% of Fe). Theoretically, Cu-Fe-ZSM-5 should be the best catalyst because there is no metal loss if we consider that every atom of each metal is active. On the other hand, Fe-Cu-ZSM-5 should be either more active than Cu-Fe-ZSM-5, if there was no loss of metal, or less active. This is because copper imposes more interactions on iron in Cu-Fe-ZSM-5 than iron does on copper in Fe-Cu-ZSM-5, as copper addition in the second step promotes the aggregation of iron species and allows to obtain a better reducibility. Normally, the catalyst with less metal content is less active, but in our case, Fe-Cu-ZSM-5 is enough active to reach the conversion of Cu-Fe-ZSM-5. Eventhough NO conversion values are more or less identical (the maximum difference is of 5±1%), catalysts behaviour are quite different due to the difference in metal species and content. Fe-Cu-ZSM-5 has certainly more active species that allowed it to compensate the metal loss. We can say that the inversion of the metal order resulted in a loss of metal and more active species, which improved the conversion of this catalyst to reach that of Cu-Fe-ZSM-5. With the same metal content, it is difficult to compare the catalysts performances because, anyway, the inversion of metal order will causes a loss in metal content and creates more active species. It also enhanced the dispersion of metal nanoparticles on the zeolite surface and stabilized a species (Fe-Cu nanocomposites) that did not exist in the solid containing more metal. Fe-Cu nanocomposites

seem to contain several active sites that were active enough to improve the activity of Fe-Cu-ZSM-5 and reach that of Cu-Fe-ZSM-5[26].

In Fe-Cu-ZSM-5, iron is mixed with copper oxide particles and Fe-O-Cu bonds of Fe-Cu nanocomposites were formed. Iron uses CuO oxygen to form Fe_2O_3 on the zeolite surface, then it migrates towards the zeolite sites. Isolated iron occupies few sites because they are already occupied by Cu as confirmed by EPR quantitative study (wt% (Fe^{3+})=0.05). Therefore, the loss of iron is conceivable as it is obtained from the species that have not found sites to occupy. Residual $FeCl_3$ will become $FeCl_3.xH_2O$ after receiving the zeolite water. The zeolite still offers water at this stage, which decreases the evaporation temperature of iron chloride so the loss of iron is certain at this stage. It can be then concluded that Fe-Cu-ZSM-5 is essentially characterized by an iron-rich surface and a copper-rich bulk.

For Cu-Fe-ZSM-5, iron migrates to the exchange sites at 290 °C. This phenomenon is facilitated by the presence of zeolite water, which promotes the diffusion of iron. At this stage, the fraction of chlorine remaining in the catalyst is very low as most of it was removed in the form of gaseous HCl. At 290 °C, the large amount of water is still available to form HCl following the reaction: $FeCl_3 + 3H_2O = Fe^{3+}(OH)_2^- + 3HCl$

This finding was confirmed by $AgNO_3$ test: a solution obtained from mixing a small amount of Cu-Fe-ZSM-5 solid and deionized water kept its initial appearance after $AgNO_3$ addition although the solution of Fe-Cu-ZSM-5 has become whitish. In fact, a dealumination was observed in ^{27}AlNMR spectrum of Cu-Fe-ZSM-5 (0 ppm-peak) as a large gaseous HCl release has occurred.

Cu-Fe-ZSM-5 contains much isolated iron as deduced from EPR quantitative study. When Copper is secondly exchanged, it will find an iron-poor surface as a large amount of iron is monomeric. Iron occupies the exchange sites, but does not establish covalent bonds with the zeolite because the SSIE temperature is low: at 290 °C, $Fe(OH)_2^+$ species occupy

$AlSiO^-$ sites but the interactions are electrostatic. After 12h, a fraction of isolated iron is stabilized (time effect not temperature effect). Indeed $Fe(OH)_2^+$ can regain the surface because it is weakly bounded to the zeolite, and it reacts with another $Fe(OH)_2^+$ to form Fe_2O_3 and water. The proof is that the catalyst Fe-ZSM-5 is not very efficient because it carries little monomeric iron. When copper is secondly exchanged, a considerable amount of isolated Cu^{2+} should be present in the exchange sites as little iron is stable at 290 °C while copper is exchanged at higher temperature, the reason why Cu^{2+} amount is higher than that of Fe^{3+}. In the catalyst Cu-Fe-ZSM-5, there is little chlorine due to the occupation of the free sites by copper.

Herein, Cu-Fe-ZSM-5 can be considered as an effective catalyst as it contains isolated species and well dispersed iron and copper oxide nanoparticles, but it also showed a dealumination where NH_3 will be oxidized to N_2O or NO_2 at strong Lewis acid sites. Fig. 2 shows that the two bimetallic catalysts exhibit the same concentration of N_2O^+ fragment, whereas in the case of Cu-Fe-ZSM-5, the concentration of the NO_2^+ fragments are more pronounced. This confirms, thus, that a dealumination has occured, which decreased the catalyst performance compared to what it would exhibit in the absence of this phenomenon.

Fe-Cu-ZSM-5 catalyst exhibits the largest amount of isolated metal species besides a better dispersion of metal nanoparticles than Cu-FeZSM-5, leading to a better accessibility of reagents (NO, O_2 and NH_3) to isolated species and then an improvement of its catalytic performances.

5. Conclusion

Fe and/or Cu exchanged ZSM-5 catalysts, prepared by solid-state ion exchange were tested in the selective catalytic reduction of NO with NH_3 in the presence of oxygen (8%) and water (3.5%). The Cu-Fe-ZSM-5 system have been studied in former works [26], the originality of this study resides in using the solid-state ion exchange as a preparation method

using low metal content (wt% =1.5). Prepared catalysts yielded more than 90% of NO conversion over a wide temperature range. The conversion's decline due to the phenomenon of ammonia oxidation did not occur in our case. A multiple-technique approach has been successfully applied to investigate of the physicochemical properties of prepared catalysts. Starting form $FeCl_3$ precursor and NH_4^+-ZSM-5 support, Fe_2O_3 nanoparticles of important size occupied the external surface of Cu-Fe-ZSM-5 along with smaller CuO nanoparticles. However, using $CuCl_2.2H_2O$ precursor in the first step of exchange, well-dispersed Fe-Cu nanocomposites species and medium-sized Fe_2O_3 particles coexist. The corresponding catalyst exhibits the larger amount of isolated species leading to the enhancement of its catalytic activity, which approximated that of Cu-Fe-ZSM-5 despite having lost a slight metal amount during the SSIE reaction. Meanwhile, a dealumination has occured in the case of Cu-Fe-ZSM-5 due to a large amount of gaseous HCl released during the preparation process thus decreasing its SCR performance to reach that of the catalyst having less metal content.

We have shown that the metal exchange order in ZSM-5 based catalysts affected the amount, degree of aggregation and environment of obtained metal species leading to a difference in catalytic behaviour in SCR reaction.

References

[1] H. Yamashita, Y. Ichihashi, S. G. Zhang, Y. Matsumura, Y. Souma, T. Tatsum, M. Anpo, Appl. Surf. Sci. 121-122 (1997)305-309.

[2]T. Ishihara, M. Ando, K. Sada, K. Takiishi, K. Yamada, H. Nishiguchi, Y. Takita, J. Catal. 220(2003)104-114.

[3] S. W. Bae, S. A. Roh, S. D. Kim, Chemosphere. 65(2006)170-175.

[4]R. Q. Long, R. T. Yang, Catal. Lett.74(2001)201-205.

[5]G. Delahay, D. Valade, A. Guzmán-Vargas, B. Coq, Appl. Catal. B: Environ.55(2005)149-155.

[6]F. Ayari, M.Mhamdi, J. Álvarez-Rodríguez, A. R. Guerrero Ruiz, G. Delahay, A. Ghorbel, Appl. Catal. B: Environ.134-135 (2013)367-380.

[7]Y. Mao, H. F. Wang, P. Hu, Int. J. Quantum Chem. 115 (2014)618-630.

[8]B. Guan, R. Zhan, H. Lin, Z. Huang, Appl. Therm. Eng. 66 (2014) 395-414.

[9]C. Capdeillayre, K. Mehsein, C. Petitto, G. Delahay, Top. Catal.59(2016)901-906.

[10]W. Arous, H. Tounsi, S. Djemel, A. Ghorbel, G. Delahay, Stud. Surf.Sci. Catal.158(2005)1883-1890.

[11]C. Torre-Abreu, C. Henriques, F. R. Ribeiro, G. Delahay, M. F. Ribeiro, Catal. Today.54(1999) 407-418.

[12]H. Sjövall, L. Olsson, E. Fridell, R. J. Blint, Appl. Catal. B: Environ. 64(2006)180-188.

[13]S. Matsumoto, K. Yokota, H. Doi, M. Kimura, K. Sekizawa, S. Kasahara, Catal.Today.22(1994)127-146.

[14]S. Kieger, G.Delahay, B. Coq, B. Neveu, J. Catal. 183(1999) 267-280.

[15]M. Moreno-Gonzalez, B. Hueso, M. Boronat, T. Blasco, A. Corma, J. Phys. Chem. Lett. 6(2015)1011-1017.

[16]P. Marturano, L. Drozdova, A. Kogelbauer, R. Prins, J. Catal. 192(2000) 236-247.

[17] J. Jia, Q. Sun, B. Wen, L. X. Chen, W. M. H. Sachtler, Catal. Lett.82 (2002) 7-11.

[18]A. A. Battiston, J. H. Bitter, F. M. F. de Groot, A. R. Overweg, O. Stephan, J. A. van Bokhoven, P. J. Kooyman, C. van der Spek, G. Vanko, D. C. Koningsberger, J. Catal. 213(2003)251-271.

[19]M. Schwidder, M. S. Kumar, K. Klementiev, M. M. Pohl, A.Brückner, W. Grünert, J. Catal. 231(2005)314-330.

[20]M. S. Kumar, M. Schwidder, W. Grünert, A.Brückner, J. Catal.227(2004) 384-397.

[21]F. Heinrich, C. Schmidt, E. Löffler, M. Menzel, W. Grünert, J. Catal. 212(2002)157-172.

[22]E. J. M. Hensen, Q. Zhu, M. M. R. M. Hendrix, A. R. Overweg, P. J. Kooyman, M. V.Sychev, R. A. van Santen, J. Catal. (2004), 221, 560-574.

[23]R. Joyner, M.Stockenhuber, J. Phys. Chem. B 103 (1999)5963-5976.

[24]F. Heinrich, C. Schmidt, E. Löffler, W. Grünert, Catal.Commun.2(2000) 317-321.

[25] H. Y. Chen, El-M.El-Malki, X. Wang, R. A. van Santen, W. M. H. Sachtler, J. Mol. Catal. A.162 (2000) 159-174.

[26]T. Zhang, J. Liu, D. Wang, Z. Zhao, Y. Wei, K. Cheng, G. Jiang, A. Duan, Appl. Catal. B: Environ.148-149 (2014)520-531.

[27]A. Sultana, M. Sasaki, K. Suzuki, H. Hamada, Catal. Commun.41(2013)21-25.

[28]P. S. Metkar, M. P. Harold, V. Balakotaiah, Appl. Catal. B: Environ.111-112 (2012)67-80.

[29]P. S. Metkar, M. P. Harold, V. Balakotaiah, Chem. Engin. Sci. 87 (2013)51-66.

[30]R. Zhang, Y. Li, T. Zhenac, RSC Adv. 4 (2014)52130-52139.

[31]P. Nakhostin, P. Panahi, D. Salari, A. Niaei, S. M. Mousavi, J. Ind. Eng. Chem. 19(2013) 1793-1799.

[32]E. Mannei, F. Ayari, M. Mhamdi, M. Almohalla, A. Guerrero. Ruiz. G. Delahay, A. Ghorbel, Micro. Meso.Mater.219(2016)77-86.

[33]I. Mejri, F. Ayari, M. Mhamdi, G. Delahay, A. Ghorbel, Z. Ksibi, Micro. Meso.Mater.220(2016)239-246.

[34] M.Høj, M. J. Beier, J. D. Grunwaldt, S. Dahl, Appl. Catal. B: Environ. 93(2009) 166-176.

[35]F. D. Liu, H.He,J. Phys. Chem. C 114(2010)16929-16936.

[36]H. W. Kouwenhoven, Adv. Chem. 121 (1973) 529-539.

[37]M. M. J. Treacy, J. B. Higgins,Collection of Simulated XRD Powder Patterns for Zeolites. Elsevier.5(2007).

[38]G. S. Qi, R. T. Yang, sur 287(2005) 25-33.

[39]N. V. Beznis, B. M. Weckhuysen, J. H. Bitter, Catal Lett. 138 (2010) 14-22.

[40] D. Ma, Y. Lu, L. Su, Z. Xu, Z. Tian, Y. Xu, L. Lin, X. Bao, J. Phys. Chem. B. 106 (2002) 8524.

[41] S.Bhatia, Zeolite Catalysis: Principles and Applications, CRC Press, Boca Raton. (1990) 75.

[42]K. Yogo, M. Umeno, H. Watanabe, K. Kikuchi, Catal. Lett.19(1993)131-135.

[43]N. Y. Topsoe, K. Pedersen, E. G. Derouane, J. Catal. 70(1981)41-52.

[44]V. H. Carmela, I. Herofumi, H. Tadasbi, M. Yuichi, J. Catal. 85(1984)362-369.

[45]H. G. Karge, Stud. Surf.Sci. Catal.65(1991)133-156.

[46] A. Jentys, A. Lugstein, H. Vinek, J. Chem. Soc. Faraday Trans. 93 (1997) 4091-4094.[47]D. R. Flentge, J. H. Lunsford, P. A. Jacobs, J. B. Uytterhoeven, J. Phys. Chem. 79 (1975)354-360.

[48]L. Xu, C. Shi , B. Chen, Q. Zhao, Micro. Meso.Mater.236 (2016) 211-217.

[49]S. Bordiga, R. Buzzoni, F. Geobaldo, C. Lamberti, E. Giamello, A. Zecchina, G. Leofanti, G. Petrini, G. Tozzola, G. Vlaic, J. Catal. 158 (1996) 486-501.

[50]A. Kubacka, Z. Wang , B. Sulikowski, J. Catal. 250 (2007) 184-189.

[51]Z. R. Ismagilov, S. A. Yashnik, V. F. Anufrienko, T. V. Larina, N. T. Vasenin, N. N. Bulgakov, S. V. Vosel, L. T. Tsykoza, Appl. Surf. Sci. 226 (2004) 88-93.

[52]M. C. N. A. de Carvalho, F.B. Passos, M. Schmal, Appl. Catal. A: Gen. 193 (2000) 265-276.

[53]C. Lamberti, S. Bordiga, M. Salvalaggio, G. Spoto, and A. Zecchina, J. Phys. Chem. B. 101(1997) 344-360.

[54]J. Dědeček, L. Čapek, B. Wichterlová, Appl. Catal. A: Gen. 307 (2006) 156-164.

[55]K. H. Rhee, F. R. Brown, D. H. Finseth, J. M. Stencel, Zeolites. 3(1983)334-347.

[56]G. Delahay, B. Coq, L. Broussous, ApplCatal. B: Environ. 12(1997)49-59.

[57]G. Delahay, D. Valade, A. Guzmán-Vargas, B. Coq, Stud. Surf.Sci. Catal. C 154 (2004)2501-2508.

[58]A. Brückner, Adv. Catal. 51(2007)265-308.

[59]M. Devadas, O. Kröcher, M. Elsener, A. Wokaun, G. Mitrikas, N. Söger, M. Pfeifer, Y. Demel, L. Mussmann, Catal.Today. 119(2007)137-144.

[60]G. Qi, R. T. Yang, Appl. Catal. B: Environ.60(2005)13-22.

[61]G. Wu, F. Hei, N. Guan, L. Li, Catal. Sci. Technol. 3 (2013)1333-1342.

Table 1

SCR operating temperatures.

Catalyst	T_{50} [a]	T_{100} [a]	SCR window [a,b]
Cu-Fe-ZSM-5	229	296	254
Fe-Cu-ZSM-5	234	335	215
Fe-ZSM-5	288	451	99
Cu-ZSM-5	267	375	175

[a] Expressed in °C, [b] Temperature range corresponding to 100% of NO conversion.

Table 2

ICP-AES chemical analysis results of as-synthesized materials.

Sample	Si/Al [a]	Fe [b]	Cu [b]	ED (%) [c]
NH_4^+-ZSM-5	15.66	-	-	-
Cu-Fe-ZSM-5	13.50	1.24	1.48	117
Fe-Cu-ZSM-5	13.16	1.16	1.36	107
Fe-ZSM-5	13.02	1.10	-	54
Cu-ZSM-5	13.88	-	1.37	44

[a] Molar ratio, [b] wt%, [c] Exchange Degree.

Table 3

NH_3-TPD and H_2-TPR results.

Sample	Acidity [a] (T_{max} [b])				Loss in strong acid sites (%)	H_2 consumption [c] (T_{max} [d])	H_2/M [e] (M=Fe or Cu)
	"l" peak	"i" peak	"h" peak	Total			
NH_4^+-ZSM-5	0.61 (217)	-	0.40 (458)	1.01	-	-	-
Cu-Fe-ZSM-5	0.47 (199)	0.19 (275)	0.15 (402)	0.81	62.50	-	-
Fe-Cu-ZSM-5	0.42 (197)	0.23 (269)	0.08 (404)	0.73	80.00	-	-
Fe-ZSM-5	0.54 (193)	0.12 (255)	0.17 (461)	0.83	57.50	0.26 (375) 0.18 (581)	1.45 1.00
Cu-ZSM-5	0.56 (198)	0.20 (268)	0.12 (415)	0.88	70.00	0.11 (371) 0.16 (478) 0.34 (620)	0.51 0.74 1.57

[a] Expressed in mmol of NH_3/g of sample, [b] Temperature of maximum desorption of low (l), intermediate (i) and high (h) peaks expressed in °C, [c] Expressed in mmol/g, [d] Expressed in°C, [e] Expressed in mol/mol.

Table 4

EPR quantitative study.

Sample	Fe^{3+}	Cu^{2+}			
	wt%	g⊥	g∥	A∥	wt%
Cu-Fe-ZSM-5	0.19	2.09	2.38	139	0.89
Fe-Cu-ZSM-5	0.05	2.09	2.37	139	1.56
Fe-ZSM-5	0.03	-	-	-	-
Cu-ZSM-5	-	2.09	2.38	137	1.14

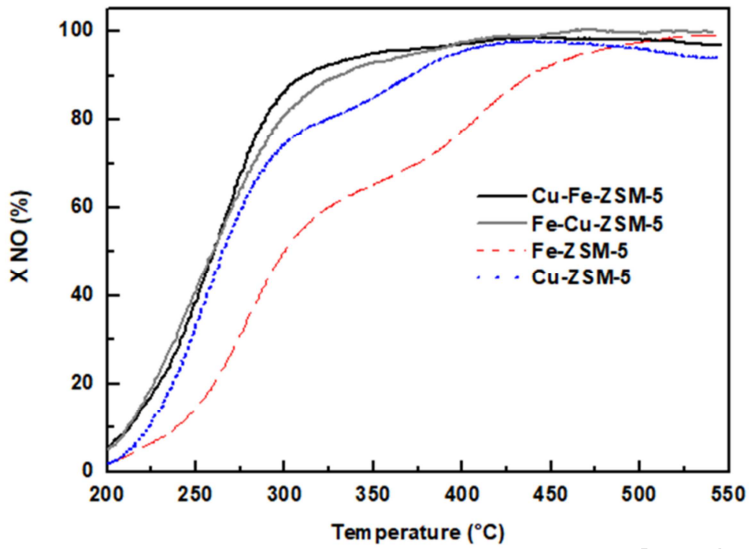

Fig.1. NO conversion over prepared catalysts.

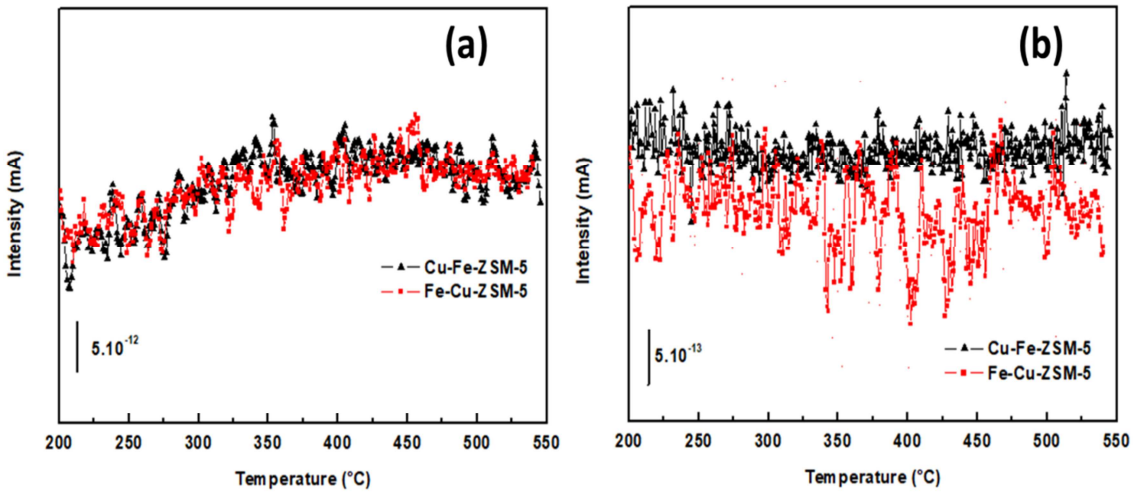

Fig. 2.Evolution of N_2O^+ fragment (m/e=44) (a) and NO_2^+ fragment (m/e=46) (b) intensities over Cu-Fe-ZSM-5 and Fe-Cu-ZSM-5 catalysts.

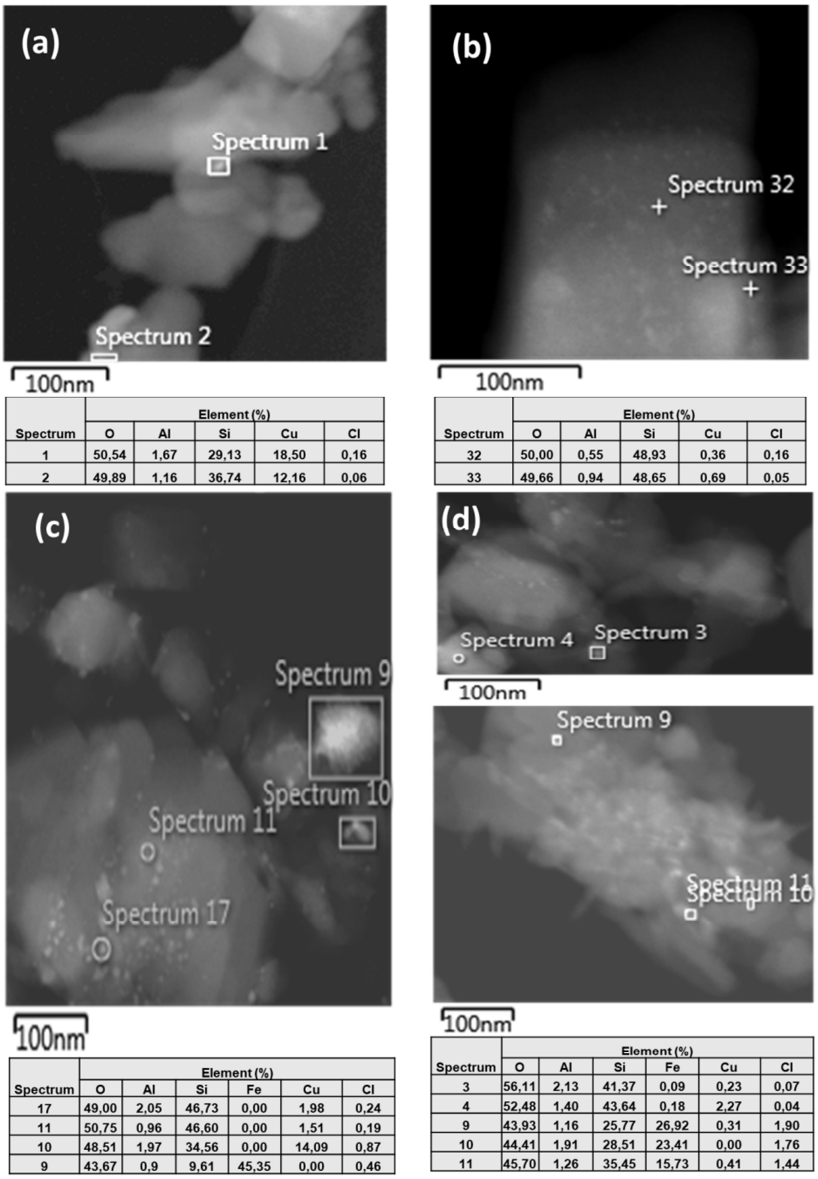

Spectrum	Element (%)				
	O	Al	Si	Cu	Cl
1	50,54	1,67	29,13	18,50	0,16
2	49,89	1,16	36,74	12,16	0,06

Spectrum	Element (%)				
	O	Al	Si	Cu	Cl
32	50,00	0,55	48,93	0,36	0,16
33	49,66	0,94	48,65	0,69	0,05

Spectrum	Element (%)					
	O	Al	Si	Fe	Cu	Cl
17	49,00	2,05	46,73	0,00	1,98	0,24
11	50,75	0,96	46,60	0,00	1,51	0,19
10	48,51	1,97	34,56	0,00	14,09	0,87
9	43,67	0,9	9,61	45,35	0,00	0,46

Spectrum	Element (%)					
	O	Al	Si	Fe	Cu	Cl
3	56,11	2,13	41,37	0,09	0,23	0,07
4	52,48	1,40	43,64	0,18	2,27	0,04
9	43,93	1,16	25,77	26,92	0,31	1,90
10	44,41	1,91	28,51	23,41	0,00	1,76
11	45,70	1,26	35,45	15,73	0,41	1,44

Fig. 3. HRTEM-STEM micrographs of Fe-ZSM-5 (a), Cu-ZSM-5 (b), Cu-Fe-ZSM-5 (c) and Fe-Cu-ZSM-5 (d).

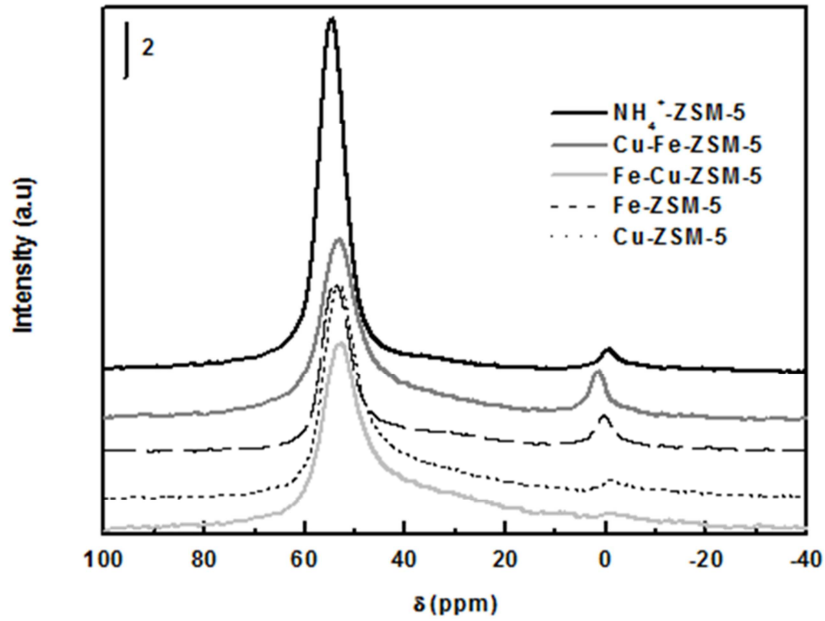

Fig. 4.[27]Al MAS NMR spectra of NH_4^+-ZSM-5 and issued catalysts.

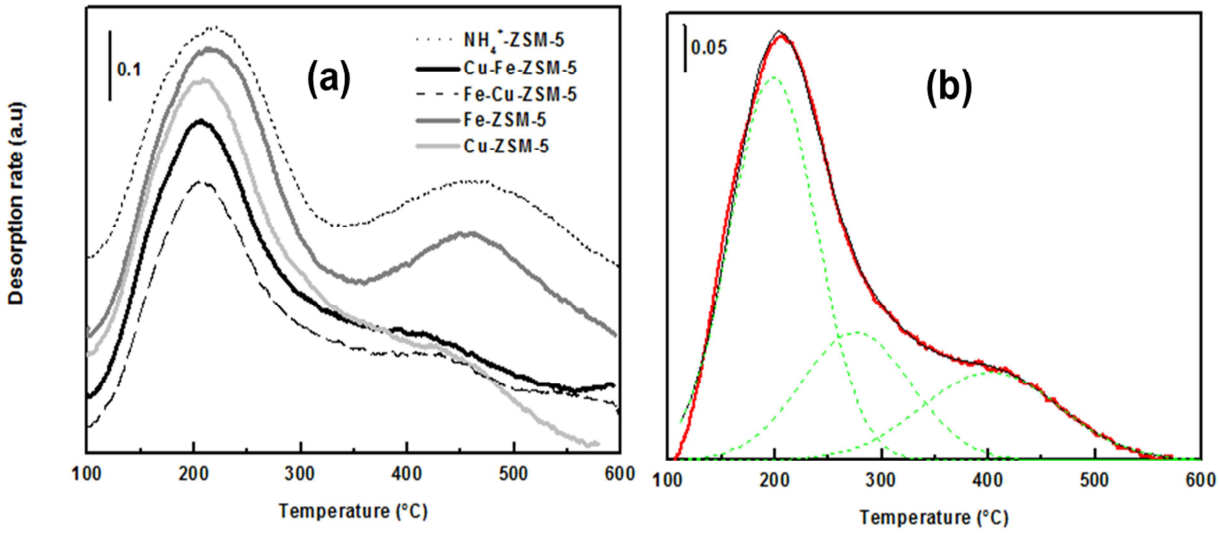

Fig. 5. NH_3-TPD profiles of NH_4^+-ZSM-5 and prepared catalysts (a) and Deconvolution of Cu-Fe-ZSM-5 TPD profile (b).

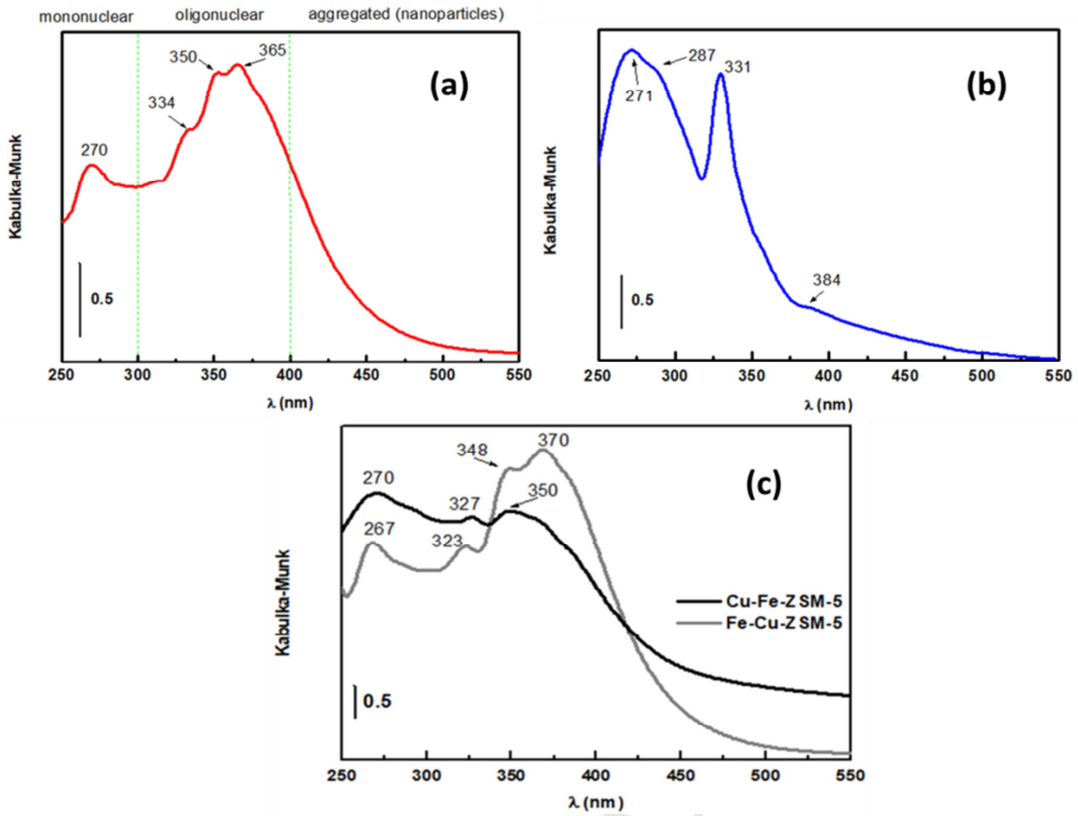

Fig. 6. DRS UV-vis spectra of Fe-ZSM-5 (a), Cu-ZSM-5 (b), Cu-Fe-ZSM-5 and Fe-Cu-ZSM-5 (c).

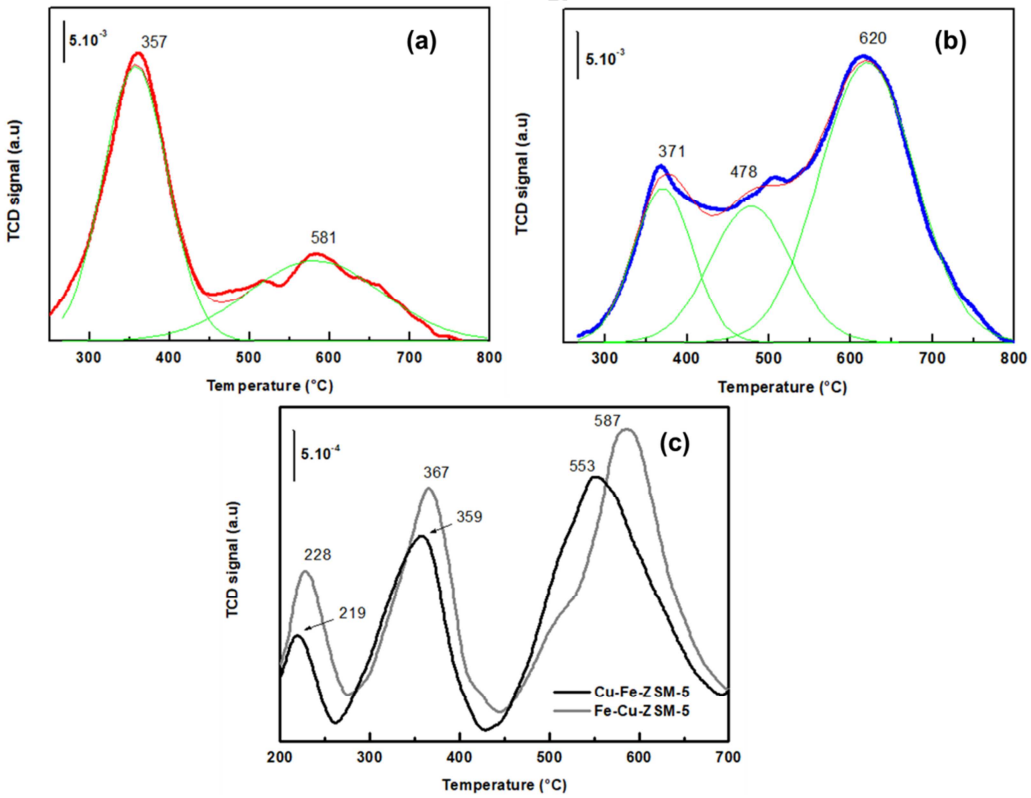

Fig. 7. H_2-TPR profiles of Fe-ZSM-5 (a), Cu-ZSM-5 (b), Cu-Fe-ZSM-5 and Fe-Cu-ZSM-5 (c).

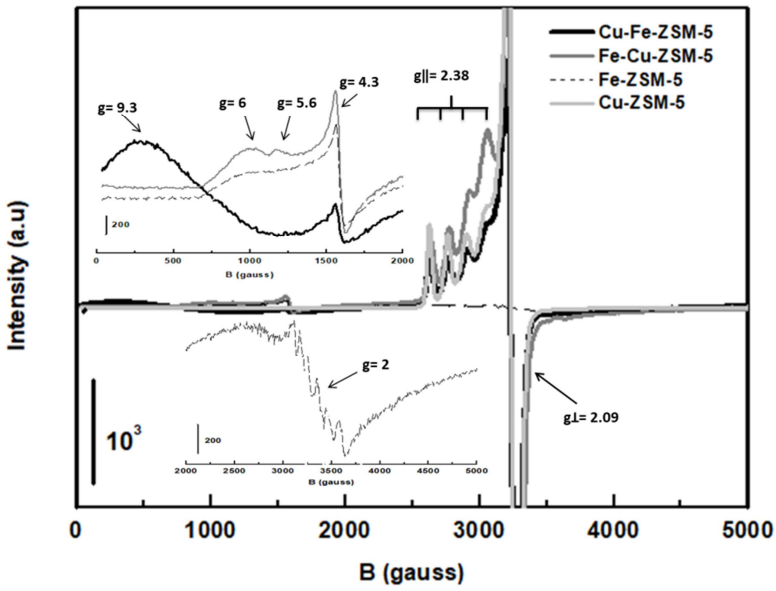

Fig.8. EPR spectra of prepared catalysts.

Research highlights

■Cu-Fe-ZSM-5 and Fe-Cu-ZSM-5 solids were prepared by solid-state ion exchange with inverting the metal exchange order.

■ Solid-state ion exchange leads to the formation of both atomically dispersed metal ions and oxide nanoparticles.

■Tested catalysts in the SCR of NO with NH_3 were active and selective towards N_2.

■The metal exchange order has a remarkable effect on the formed metal species and the catalytic behavior of the studied catalyst.